

000
001
002
003
004
005
006
007
008
009
010
011
012
013
014
015
016
017
018
019
020
021
022
023
024
025
026
027
028
029
030
031
032
033
034
035
036
037
038
039
040
041
042
043
044
045
046
047
048
049
050
051
052
053

054
055
056
057
058
059
060
061
062
063
064
065
066
067
068
069
070
071
072
073
074
075
076
077
078
079
080
081
082
083
084
085
086
087
088
089
090
091
092
093
094
095
096
097
098
099
100
101
102
103
104
105
106
107

Self-Supervised Deep Visual Odometry with Online Adaptation

— Supplementary Material —

Anonymous CVPR submission

Paper ID 2089

1. Network Architecture

The detailed network architectures of DepthNet, PoseNet and MaskNet are shown in Table 1, 2, 3. All convolutions, deconvolutions and convLSTM are followed by layer normalization (LN) and ReLU activation except for the output layer.

2. Analysis of online adaptation for VO

The problem of online adaptation for VO is very hard, especially when we require that the estimated trajectory in the unseen environment should be close to the ground truth.

Despite some recent works on stereo matching and stereo depth estimation [5, 4, 3] claim that they are able to get reasonable matching and depth in unseen environments after hundreds of online refinement process, these methods use stereo images and the baselines between two cameras are known, which significantly simplifies the online learning problem. In contrast, our method uses only monocular images and the relative pose between consecutive images are unknown. The network needs to adapt online for better pose and depth estimation simultaneously, which is much harder than stereo matching or depth estimation.

Besides, even if the VO network adapts to the new environment after hundreds of updating (maybe 500-2000 frames), previous estimations still have large errors. As the errors are accumulated, the trajectories are getting more and more drifted with time (shown in Fig. 2). This indicates that in order to get a better trajectory, the estimation error should be small at the *beginning* of online adaptation, and the network has to adapt itself as *fast* as possible so as to reduce accumulated error. It can be seen from Fig. 2 that our method achieves promising online adaptation performance compared with other baselines. We select some complicated and challenging trajectories from KITTI [2] 00-10, including multiple turns, loops and sharp turns. If the pose estimation goes wrong at one turn, the trajectory will drift afterwards, no matter how accurate it estimates later. These results demonstrate that our method is able to get small estimation error at the beginning of domain shift, and adapts

quickly to the new environment.

3. Pretrain on Carla

We use Carla [1] simulator to create virtual images under different conditions in the virtual city (shown in Fig. 1). We use these collected images to pretrain our network together with other baselines, and test them on KITTI odometry [2] dataset. The results are shown in Fig. 2.

References

- [1] Alexey Dosovitskiy, German Ros, Felipe Codevilla, Antonio Lopez, and Vladlen Koltun. CARLA: An open urban driving simulator. In *Proceedings of the 1st Annual Conference on Robot Learning*, pages 1–16, 2017. 1, 3
- [2] Andreas Geiger, Philip Lenz, and Raquel Urtasun. Are We Ready for Autonomous Driving? The KITTI Vision Benchmark Suite. In *CVPR*, 2012. 1
- [3] Alessio Tonioni, Matteo Poggi, Stefano Mattoccia, and Luigi Di Stefano. Unsupervised adaptation for deep stereo. In *ICCV*, 2017. 1
- [4] Alessio Tonioni, Oscar Rahnama, Thomas Joy, Luigi Di Stefano, Thalaiyasingam Ajanthan, and Philip HS Torr. Learning to Adapt for Stereo. In *CVPR*, 2019. 1
- [5] Alessio Tonioni, Fabio Tosi, Matteo Poggi, Stefano Mattoccia, and Luigi Di Stefano. Real-Time Self-Adaptive Deep Stereo. In *CVPR*, 2019. 1
- [6] Tinghui Zhou, Matthew Brown, Noah Snavely, and David G Lowe. Unsupervised Learning of Depth and Ego-Motion from Video. In *CVPR*, 2017. 2

108					162
109					163
110					164
111	Block	Operation	Filter size	Stride	Output size (height×width×channel)
112	Input I				128×416×3
113		Convolution	7×7	2	64×208×32
114		Convolution	7×7	1	64×208×32
115		Convolution	5×5	2	32×104×64
116		Convolution	5×5	1	32×104×64
117		Convolution	3×3	2	16×52×128
118		Convolution	3×3	1	16×52×128
119	Encoder	Convolution	3×3	2	8×26×256
120		Convolution	3×3	1	8×26×256
121		ConvLSTM	3×3	1	8×26×256
122		Convolution	3×3	2	4×13×256
123		Convolution	3×3	1	4×13×256
124		ConvLSTM	3×3	1	4×13×256
125		Convolution	3×3	2	2×7×512
126		Convolution	3×3	1	2×7×512
127		ConvLSTM	3×3	1	2×7×512
128					179
129		Deconvolution	3×3	2	4×13×512
130		Concatenation	-	-	4×13×768
131		Convolution	3×3	1	4×13×512
132		Deconvolution	3×3	2	8×26×256
133		Concatenation	-	-	8×26×512
134		Convolution	3×3	1	8×26×256
135		Deconvolution	3×3	2	16×52×128
136		Concatenation	-	-	16×52×256
137		Convolution	3×3	1	16×52×128
138		Convolution	3×3	1	16×52×1
139		Sigmoid (get disparity d_1)	-	-	16×52×1
140		$d_1 = 100 \times d_1 + 0.01$	-	-	16×52×1
141	Decoder	Deconvolution	3×3	2	32×104×64
142		Bilinear upsampling from d_1	-	2	32×104×1
143		Concatenation	-	-	32×104×129
144		Convolution	3×3	1	32×104×64
145		Convolution	3×3	1	32×104×1
146		Sigmoid (get disparity d_2)	-	-	32×104×1
147		$d_2 = 100 \times d_2 + 0.01$	-	-	32×104×1
148		Deconvolution	3×3	2	64×208×32
149		Bilinear upsampling from d_2	-	2	64×208×1
150		Concatenation	-	-	64×208×65
151		Convolution	3×3	1	64×208×32
152		Convolution	3×3	1	64×208×1
153		Sigmoid (get disparity d_3)	-	-	64×208×1
154		$d_3 = 100 \times d_3 + 0.01$	-	-	64×208×1
155		Deconvolution	3×3	2	128×416×32
156		Bilinear upsampling from d_3	-	2	128×416×1
157		Concatenation	-	-	128×416×65
158		Convolution	3×3	1	128×416×32
159		Convolution	3×3	1	128×416×1
160		Sigmoid (get disparity d_4)	-	-	128×416×1
161		$d_4 = 100 \times d_4 + 0.01$	-	-	128×416×1
162	Output d_4				128×416×1
163					210
164					211
165					212
166					213
167					214
168					215

Table 1. Detailed DepthNet architecture, which is basically the same as the DepthNet of SfMLearner [6] but much more lightweighted. The output is disparity d_4 (inverse depth). Then depth $\hat{D} = \frac{1}{d_4}$.

Block	Operation	Filter size	Stride	Output size (height×width×channel)
Input $I_t, \hat{D}_t, I_{t-1}, \hat{D}_{t-1}$				128×416×8
Shared encoder	Convolution	7×7	2	64×208×16
	ConvLSTM	3×3	1	64×208×16
	Convolution	5×5	2	32×104×32
	ConvLSTM	3×3	1	32×104×32
Translation estimation t_x, t_y, t_z	Convolution	3×3	2	16×52×64
	ConvLSTM	3×3	1	16×52×64
	Convolution	3×3	1	16×52×3
	Fully Connected	-	-	1×1×3
Rotation estimation r_x, r_y, r_z	Convolution	3×3	2	16×52×64
	ConvLSTM	3×3	1	16×52×64
	Convolution	3×3	1	16×52×3
	Fully Connected	-	-	1×1×3
Output 6-DoF pose $t_x, t_y, t_z, r_x, r_y, r_z$				1×1×6

Table 2. Detailed PoseNet architecture.

Block	Operation	Filter size	Stride	Output size (height×width×channel)
Input warping residual				128×416×3
Encoder	Convolution	7×7	1	128×416×16
	Convolution	5×5	1	128×416×32
	Convolution	5×5	1	128×416×32
	Convolution	3×3	1	128×416×1
	Sigmoid	-	-	128×416×1
Output mask \hat{M}				128×416×1

Table 3. Detailed MaskNet architecture.

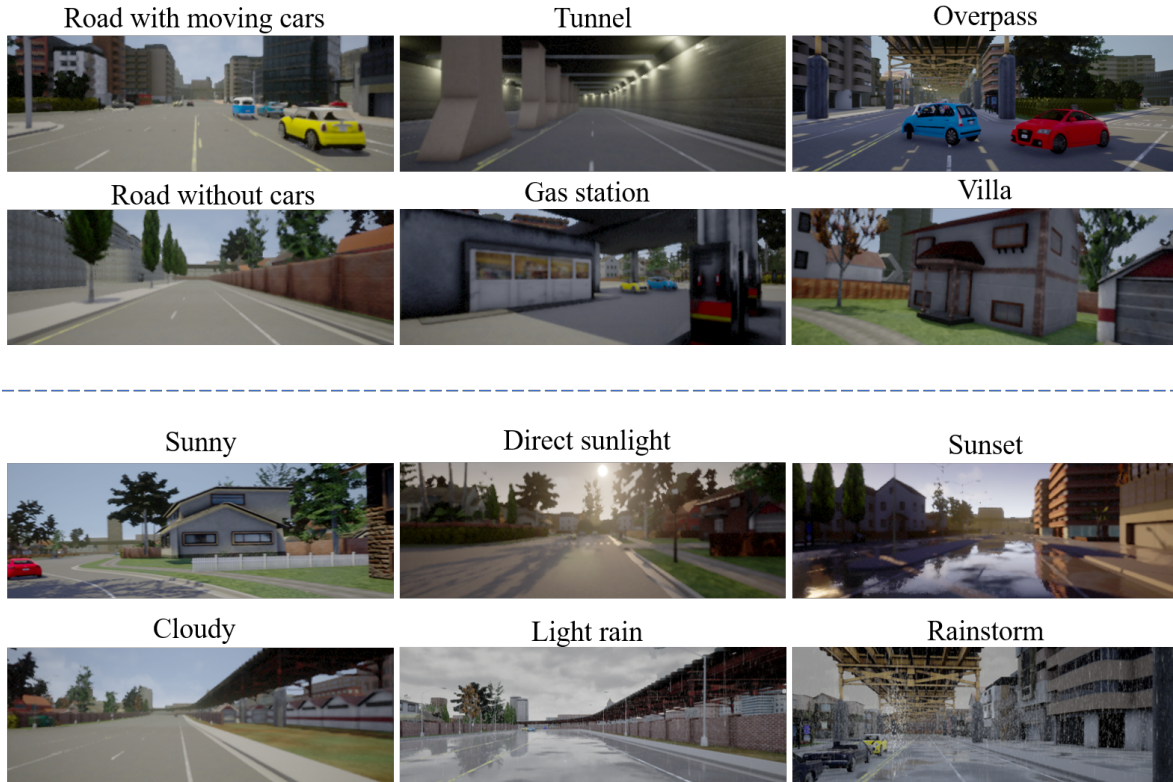


Figure 1. Different types of scenes we collected by Carla [1] simulator.

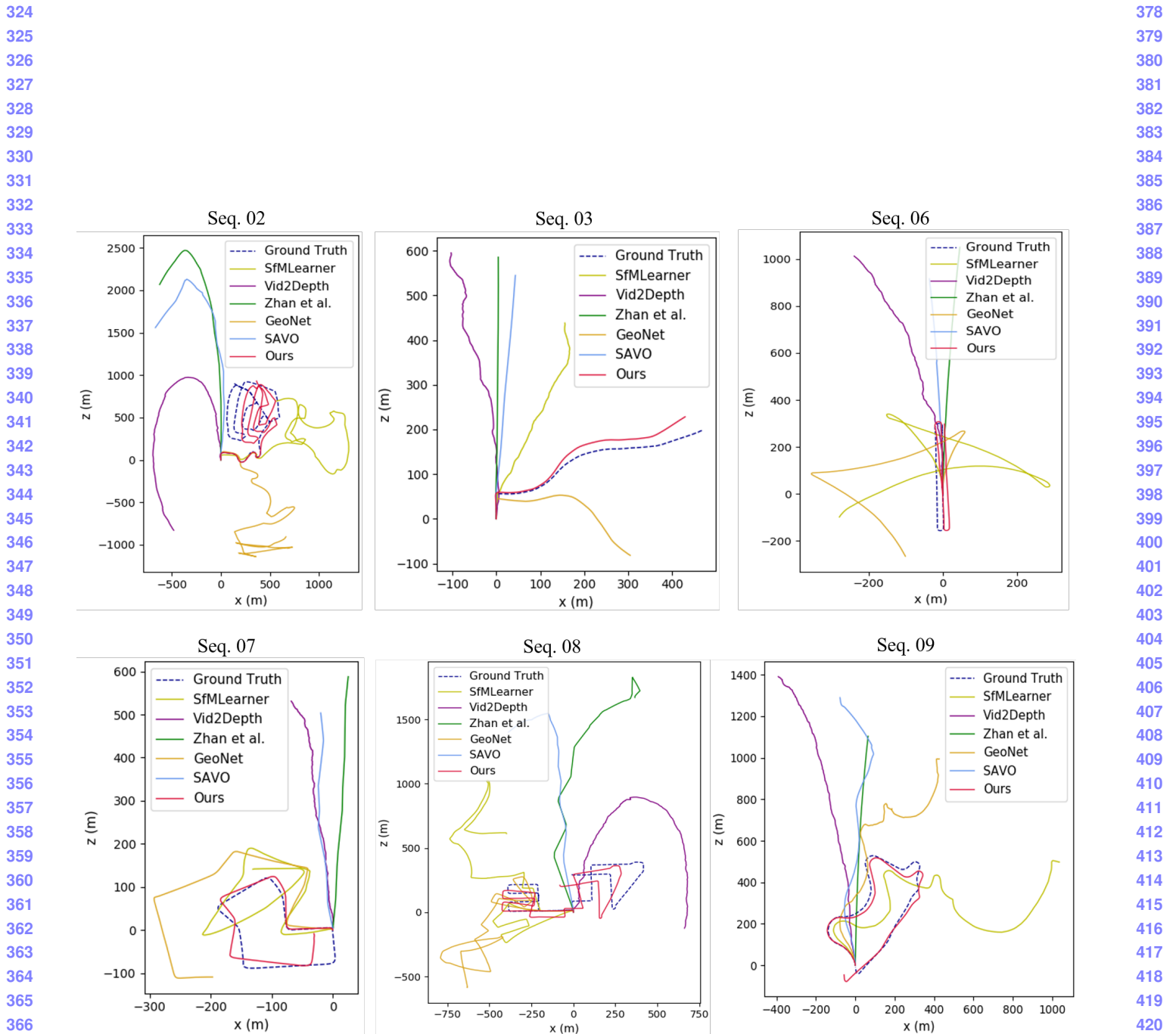


Figure 2. Results of various methods pretraining on Carla and online testing on KITTI 00-10. We select some complicated and challenging trajectories from these 11 sequences, including multiple turns, loops and sharp turns.